



Transient responses to increasing CO₂ and climate change in an unfertilized grass–clover sward

Patrick Lazzarotto¹, Pierluigi Calanca^{1,*}, Mikhail Semenov², Jürg Fuhrer¹

¹Agroscope Reckenholz-Tänikon Research Station ART, Air Pollution/Climate Group, Reckenholzstrasse 191, 8046 Zurich, Switzerland

²Centre for Mathematical and Computational Biology, Rothamsted Research, Harpenden, Hertfordshire AL5 2JQ, UK

ABSTRACT: Mechanisms controlling transient responses to elevated CO₂ concentration and climate change in an unfertilized grassland on the Swiss Plateau were examined in light of simulations with PROGRASS, a process-based model of grass–clover interactions. Daily weather for a series of transient climate scenarios spanning the 21st century were developed for the study site with the help of the LARS-WG weather generator. Changes in the length of dry and wet spells, temperature, precipitation and solar radiation defining the scenarios were obtained from regional climate simulations carried out in the framework of the PRUDENCE project. Compared to 1961–1990, the latter indicated that for 2071–2100 there would be a noticeable increase in temperature (roughly 3°C in winter and 5°C in summer), a significant drop in summer precipitation (of the order of –30%) and a nearly 2-fold increase in the length of dry spells. Assuming that clover is less drought-tolerant than grass, we examined whether clover abundance would decrease as a consequence of increasing heat and water stress, or be promoted on account of CO₂ stimulation. Results indicated that: (1) at our site, climate change alone did not curtail biological N₂ fixation to the point as to alter the composition of the sward but nevertheless entailed a decrease in grassland productivity; (2) increasing CO₂ clearly promoted clover growth (via feedbacks on nitrogen acquisition) and grassland productivity; and (3) even with CO₂ stimulation, the additional N input from symbiotic N₂ fixation was not sufficient to substantially improve the mineral N status of the system and promote grass competitiveness.

KEY WORDS: Climate change · Elevated CO₂ · Grassland productivity · Biological N₂ fixation · Grass–clover interactions · Transient responses

Resale or republication not permitted without written consent of the publisher

1. INTRODUCTION

Management of grasslands for herbage yield represents an essential aspect of farm economies in Europe and elsewhere (Whitehead 1995). Grasslands are also major reservoirs of soil organic matter (SOM) (Schimel 1995) and thus play an important role in the terrestrial carbon (C) cycle. Assessing possible responses of grasslands to climate change is therefore an important step towards identifying adaptation needs to secure grassland services.

Free-air carbon dioxide enrichment (FACE) experiments (e.g. Schneider et al. 2004) and modelling studies (Hunt et al. 1991, 1998, Parton et al. 1995, Thornley & Cannell 1997, Riedo et al. 1999) have indicated that grassland productivity may benefit from increas-

ing atmospheric CO₂ concentrations. This could result from the direct stimulation of photosynthetic C assimilation, although recently there has been some controversy about the magnitude of this effect (Long et al. 2006), but also improved water use efficiency (e.g. Volk et al. 2000). However, the positive response to elevated CO₂ may be opposed by feedback mechanisms associated with nutrient cycling (Diaz et al. 1993, Rastetter et al. 1997). In particular, shifts in the balance between nitrogen (N) mineralisation and immobilization in favour of the latter (Thornley & Cannell 2000, Shaw et al. 2002, Hu et al. 2006) could restrict the availability of soil N and, consequently, plant photosynthetic capacity or sink activity. This effect could be most important in unfertilized grasslands (de Graaff et al. 2006) or in systems where N

*Corresponding author. Email: pierluigi.calanca@art.admin.ch

inputs are essentially limited to biological N₂ fixation (BNF) by legumes.

In this context, it is worth recalling that much of the world's grasslands are botanically diverse. The response of functional groups and individual species within a sward is therefore of interest, as changes in these components can alter nutrient cycling and affect biodiversity (Lüscher et al. 2005). In view of a limited understanding of long-term changes in nutrient cycling, shifts in the botanical composition remain uncertain.

White clover *Trifolium repens* L. is the most important pasture legume grown in temperate climates in association with a variety of grasses, notably perennial ryegrass *Lolium perenne* L. White clover improves the nutritional quality and digestibility of the herbage. In addition, it contributes substantially to the N status of the sward through BNF. A positive response of the latter to elevated CO₂ (Zanetti et al. 1996, Hebeisen et al. 1997) may thus help sustain productivity even when climatic conditions become otherwise unfavourable. Still, this ultimately depends on the long-term competitive success of clover in mixture with grasses.

In modelling studies, the coexistence of grass and clover in mixed swards has been investigated mostly from a theoretical point of view (Ross et al. 1972, Thornley et al. 1995, Schwinning & Parsons 1996a,b, Louie et al. 2002, Schulte 2003, Schulte et al. 2003), but have largely been ignored in impact assessments (Parton et al. 1995, Topp & Doyle 1996, Thornley & Cannell 1997, 2000, Riedo et al. 1999). This situation is clearly unsatisfactory and prompted us to undertake an attempt to include dynamic grass–clover interactions in the analysis of the effects of elevated CO₂ and climate change on an unfertilized grassland ecosystem.

Our work was based on the application of the Productive Grassland Simulator (PROGRASS, Lazzarotto et al. 2009) to an extensively managed sward located on the Swiss Central Plateau. Climate scenarios for the 21st century were developed for our study site on the basis of results from the Prediction of Regional scenarios and Uncertainties for Defining European Climate change risks and Effects (PRUDENCE) project (Christensen & Christensen 2007). Contrary to studies that assume a step change in climate and atmospheric CO₂ or examine equilibrium responses, here the focus was on transient simulations on the background of continuously evolving atmospheric CO₂ and climatic conditions.

For our location, the scenarios indicated a higher incidence of heat stress and drought conditions during late spring, summer and early autumn. We conjectured that this would have implications for grassland composition because white clover is considered to respond more strongly to drought than perennial ryegrass (Frame & Newbould 1986). On the other hand, field experiments have suggested that white clover could profit more than

ryegrass from elevated CO₂ concentration (Hebeisen et al. 1997), implying a trade-off between positive and negative impacts that remains to be quantified.

Based on these considerations, our work focused on testing 2 contrasting hypotheses: (1) increasing heat and water stress will lead to a decline in clover abundance over time, in particular if grass can profit from the emerging competitive advantages with respect to C assimilation and N acquisition (Lazzarotto et al., 2009); (Lazzarotto et al. 2009); (2) in the long term, the negative impacts of climate change on clover will be offset by the benefits of elevated CO₂ on BNF (Zanetti et al. 1996, Serraj et al. 1998), promoting clover growth and grassland productivity.

2. MATERIALS AND METHODS

2.1. Experimental site and field data. The data were collected from an experiment running since 2001 on the Swiss Central Plateau at Oensingen (7° 44' E, 47° 17' N, 450 m above sea level [a.s.l.]). At this site, annual mean temperature is 0.5°C and annual precipitation is 1100 mm, with 55 % of the total amount falling between April and September and 30 % between June and August.

The grassland system was established in 2001 following conversion from a long-term arable rotation (Ammann et al. 2009) on a stagnic cambisol (eutric) with sand, silt and clay fractions of 0.25, 0.32 and 0.43, respectively, and a pH of 7.3. Undergoing extensive management, the field was harvested 3 times each year without the addition of fertilizers. Volumetric soil water contents at saturation (0.53 m³ m⁻³), field capacity (0.46 m³ m⁻³) and permanent wilting point (0.31 m³ m⁻³) were determined on soil cores using standard methods. A saturated soil hydraulic conductivity of 410 mm d⁻¹ was estimated using ROSETTA software (Schaap et al. 2001), assuming a relatively low bulk density of 1.16 × 10⁶ g m⁻³.

In 2001, the organic N content in the top 20 cm was 0.82 kg m⁻². This value exceeds the range (0.25 to 0.75 kg m⁻²) that can be inferred for temperate grasslands from data collected by Jobbágy & Jackson (2000) and assuming a C:N ratio in SOM of about 10 (Conant et al. 2005). This suggests that our study site is not necessarily representative of semi-natural systems.

The floristic composition of the sward was estimated annually by a visual survey using the method of Braun-Blanquet (1964). Average clover fraction throughout the growing season was between 0.5 and 0.6.

2.2. The model. A detailed description of PROGRASS has recently been published by Lazzarotto et al. (2009). In brief, plant processes (including C assimilation, plant respiration, mineral N uptake, BNF, allocation of assimilates to shoot and root compartments,

and senescence) were simulated by PROGRASS separately for grass and clover. Light relations were modelled assuming a higher extinction coefficient for clover (0.8) than for grass (0.5). Mineral N uptake rates and BNF depended on soil mineral N availability. Further, the model assumed plant-specific responses to temperature, soil water availability and atmospheric CO₂. Inputs to the SOM pool were from plant decay and fertilization, while outputs were linked with mineralization. Apart from N uptake by the plants, the mineral N pool was depleted by leaching and gaseous N exchange with the atmosphere.

As mentioned in Lazzarotto et al. (2009), values for the model parameters were either taken from the literature or determined from an application of PROGRASS to the FACE experiment run at Eschikon, Switzerland (47° 27' N, 8° 41' E, 550 m a.s.l.) (Hebeisen et al. 1997).

For the present study, the model was extended with respect to the computation of SOM turnover, BNF and soil temperature. Concerning SOM dynamics, the original formulation was replaced by the set of equations implemented in the CENTURY model (Parton et al. 1987, 1993). This modification entailed a partitioning of the N losses into gaseous emissions and leaching of organic and mineral N.

With respect to BNF, we introduced a new response function, $f_{\text{BNF}}^{\theta, \text{CO}_2}(\theta, c_a)$, that simultaneously accounts for water status (θ) and atmospheric CO₂ (c_a) according to the experimental results of Serraj et al. (1998). The equation for the BNF rate, U_{BNF} , is therefore:

$$U_{\text{BNF}} = f_{\text{BNF}}^{\text{T}}(T_s) f_{\text{BNF}}^{\theta, \text{CO}_2}(\theta, c_a) e_{\text{BNF}} U_{\text{BNFmax}} W_{\text{rt,c}} \left(1 - f_{\text{Uc}} \frac{N_{\text{min}}}{N_{\text{min}} + \kappa_{\text{BNF}}} \right) \quad (1)$$

where $f_{\text{BNF}}^{\text{T}}(T_s)$ expresses the dependence of BNF on soil temperature T_s , $W_{\text{rt,c}}$ is the root dry matter (DM) of clover, N_{min} the soil mineral N content, $e_{\text{BNF}} = 0.5$ the BNF efficiency relative to soil mineral N uptake, $U_{\text{BNFmax}} = 0.0024 \text{ kg N (kg root DM)}^{-1} \text{ d}^{-1}$ the maximal BNF rate, $f_{\text{Uc}} = 0.95$ the maximal fraction of N uptake from the soil, and $\kappa_{\text{BNF}} = 0.006 \text{ kg N}_{\text{min}} \text{ m}^{-2}$ the soil mineral N content at which the BNF rate becomes half-maximal. Moreover,

$$f_{\text{BNF}}^{\theta, \text{CO}_2}(\theta, c_a) = \begin{cases} 1 & \text{if } \theta > \theta_{\text{ws,BNF}}(c_a) \\ f_{\text{BNF,min}}^{\theta}(c_a) + \left[1 - f_{\text{BNF,min}}^{\theta}(c_a) \right] \frac{\theta - \theta_{\text{pwp}}}{\theta_{\text{ws,BNF}}(c_a) - \theta_{\text{pwp}}} & \text{if } \theta_{\text{pwp}} < \theta \leq \theta_{\text{ws,BNF}}(c_a) \\ f_{\text{BNF,min}}^{\theta}(c_a) & \text{if } \theta \leq \theta_{\text{pwp}} \end{cases} \quad (2)$$

where $f_{\text{BNF,min}}^{\theta}$ and $\theta_{\text{ws,BNF}}$ are given by Eqs. (4) & (5), respectively, θ_{pwp} denotes the soil water content at the permanent wilting point and as before:

$$f_{\text{BNF}}^{\text{T}}(T_s) = \begin{cases} 0 & \text{if } T_s \leq T_{\text{BNF,1}} \\ (T_s - T_{\text{BNF,1}})/(T_{\text{BNF,2}} - T_{\text{BNF,1}}) & \text{if } T_{\text{BNF,1}} < T_s \leq T_{\text{BNF,2}} \\ 1 & \text{if } T_{\text{BNF,2}} < T_s \leq T_{\text{BNF,3}} \\ 1 - [(T_s - T_{\text{BNF,3}})/(T_{\text{BNF,4}} - T_{\text{BNF,3}})] & \text{if } T_{\text{BNF,3}} < T_s \leq T_{\text{BNF,4}} \\ 0 & \text{if } T_{\text{soil}} > T_{\text{BNF,4}} \end{cases} \quad (3)$$

with parameters $T_{\text{BNF,1}} = 9^\circ\text{C}$, $T_{\text{BNF,2}} = 13^\circ\text{C}$, $T_{\text{BNF,3}} = 26^\circ\text{C}$ and $T_{\text{BNF,4}} = 30^\circ\text{C}$.

In Eq. (2) the fraction of BNF that can be maintained at the permanent wilting point is given by:

$$f_{\text{BNF,min}}^{\theta}(c_a) = f_{\text{E,min}}^{\theta} \left[\frac{1 + c_{\text{gs}}}{1 + (c_{\text{gs}} c_a / c_{350})} \right]^{-1} \quad (4)$$

where $f_{\text{E,min}}^{\theta} = 0.4$ and $c_{\text{gs}} = 2$ is a dimensionless parameter controlling the effects of atmospheric CO₂ on stomatal conductance. Similarly, the soil water content at which BNF starts to be limited by water stress is calculated as:

$$\theta_{\text{ws,BNF}}(c_a) = \theta_{\text{pwp}} + (\theta_{\text{ws,c}} - \theta_{\text{pwp}}) \left[\frac{1 + c_{\text{gs}}}{1 + (c_{\text{gs}} c_a / c_{350})} \right] \quad (5)$$

Here $\theta_{\text{ws,c}}$ is the soil water content at incipient stomatal closure. It is calculated from the corresponding soil water potential $\psi_{\text{ws,c}} = -400 \text{ J kg}^{-1}$ according to Campbell (1985) as:

$$\theta = \theta_{\text{sat}} \left(\frac{\psi_e}{\psi_{\text{ws,c}}} \right)^{1/b} \quad (6)$$

where θ_{sat} is the volumetric soil water content at saturation and ψ_e the so-called air entry potential that, along with the shape parameter b , depends on soil physical properties.

At $c_a = 350 \text{ ppm}$, $f_{\text{BNF,min}}^{\theta}(c_a)$ from Eq. (4) is equal to $f_{\text{E,min}}^{\theta} = 0.4$, increasing almost linearly with c_a above this threshold to reach a value of about 0.8 at $c_a = 860 \text{ ppm}$. Likewise, $\theta_{\text{ws,BNF}}(c_a)$ is equal to $\theta_{\text{ws,c}}$ at $c_a = 350 \text{ ppm}$, and decreases with increasing c_a to half this value at $c_a = 860 \text{ ppm}$.

Concerning the evaluation of soil temperature, the minimalistic scheme considered by Lazzarotto et al. (2009) was improved as followed. We first calculated variations in soil temperature associated with the annual cycle of air temperature (T_{sA}) using the analytical solution of the heat conduction equation for a homogeneous, semi-infinite soil slab subject to harmonic boundary conditions (e.g. Carslaw & Jaeger 1959), namely:

$$T_{\text{sA}}(z, t) = M_A + A_A \exp\left(-\frac{z}{z_{\text{DA}}}\right) \sin(\omega_A t + \Phi_A - z/z_{\text{DA}}) \quad (7)$$

where M_A , A_A and Φ_A are respectively the mean, amplitude and phase of the annual cycle, $\omega_A = 2\pi/365 \text{ d}^{-1}$ the angular frequency, $z_{\text{DA}} = (2D/\omega_A)^{1/2}$ the so-called

damping depth, and z the effective depth, assumed to be 0.2 m. As seen here, the damping depth is related to the thermal diffusivity D which itself is a function of soil texture and water content (Campbell 1985).

Next, we computed the difference between surface radiation temperature, T_{OR} , and air temperature, T_{a} , according to Holtslag & van Ulden (1983) as:

$$\delta T_{\text{OR}} = T_{\text{OR}} - T_{\text{a}} \equiv \frac{c_{\text{R}} \text{NR}}{4\sigma T_{\text{a}}^3} f_{\text{LAI}} \quad (8)$$

where

$$f_{\text{LAI}} = \exp(-\kappa_{\text{e}} \text{LAI}) \quad (9)$$

In Eq. (8), NR is the surface radiation budget estimated from incoming solar radiation (Davies 1967), c_{R} a heating coefficient of the order of 0.1 (Monteith & Szeicz 1961), $\sigma = 5.67 \times 10^{-8} \text{ W m}^{-2} \text{ K}^{-4}$ the Stefan-Boltzmann constant, while in Eq. (9) κ_{e} is the effective extinction coefficient of the canopy (Lazzarotto et al. 2009) and LAI the total leaf-area index.

A basic assumption underlying our revised algorithm was that δT_{OR} reflects the dominant mode of variability at time scales between the daily and the seasonal. Spectral analysis of temperature records at our study site suggested that the dominant mode of variability has a periodicity of $2\pi/\omega_{\text{m}} \approx 14 \text{ d}$, ω_{m} being the corresponding circular frequency. Defining $z_{\text{Dm}} = (2\kappa/\omega_{\text{m}})^{1/2}$, introducing the time delay implicitly and using the surface temperature anomaly given by Eq. (8) to perturb $T_{\text{sA}}(z, t)$ from Eq. (7), the daily soil temperature T_{s} was finally calculated as:

$$T_{\text{s}}(z, t + \frac{z/z_{\text{Dm}}}{\omega_{\text{m}}}) = T_{\text{sA}}(z, t) + \delta T_{\text{OR}}(t) \exp\left(-\frac{z}{z_{\text{Dm}}}\right) \quad (10)$$

2.3. LARS-WG weather generator. Climate scenarios for the study sites were generated using the LARS-WG stochastic weather generator (Semenov & Barrow 1997, Semenov et al. 1998). LARS-WG relies on the serial approach to the analysis of weather series developed by Racsko et al. (1991) and uses the normal distribution to model temperature variables (with mean and standard deviation varying daily according to finite 3rd order Fourier series) and semi-empirical distributions to model precipitation and solar radiation, separately on wet and dry days (Semenov 2007).

The standard procedure to construct daily weather for a climate change scenario consists of 2 steps (Semenov, 2007). First, parameters defining the statistical distributions of minimum and maximum temperature, precipitation and solar radiation are computed for the baseline period using long-term weather observations. In our case we used daily data for 1981–2007 from an operational weather station (Wynau, $7^{\circ}47' \text{ E}$, $47^{\circ}15' \text{ N}$, 422 m a.s.l.) located approximately 5 km southeast of our study site. The performance of LARS-WG for our site was examined on the basis of statistical

tests built in the weather generator (χ^2 goodness-of-fit tests for comparing probability distributions; t - and F -tests for comparing mean values and standard deviations). Overall, the tests indicated a high likelihood ($p > 0.01$) that observed and synthetic data stem from the same population. In the second step, the climate change signal extracted from global or regional climate simulations (scenario versus baseline) is used to modify the baseline statistical parameters. This requires specification of changes in average monthly values for total precipitation, minimum and maximum temperature, interannual variability of mean temperature, solar radiation and duration of wet and dry spells. In the standard version, the new statistics are directly used by LARS-WG to generate daily data under the assumption of a new stationary state.

For our application, LARS-WG was modified to enable the generation of daily data reflecting evolving climate conditions. As before, changes in monthly statistics were specified for the end of a period of interest (in our case anomalies for the year 2100). These were linearly interpolated in time to obtain a transient evolution of the climate change signal, and it was only at this stage that synthetic daily data were created. This procedure ensures a smooth transition from year to year.

One may argue that the assumption of a linear trend for the climate change signal is not realistic. Departures from linearity indeed appear in global and regional climate simulations but, if at all, they are of concern only relatively to the last decades of the 21st century. In view of the many other uncertainties affecting the scenarios (assumptions concerning the emissions scenario, choice of global and regional climate model, specific setup of the corresponding simulations), we maintain that the approach can be justified.

2.4. Estimation of hourly data. Hourly data needed as model input were derived in the post-processing of LARS-WG outputs following Thornley & France (2007). For radiation, a weighted average of a full sine and half sine curve were used to mimic the diurnal cycle, whereas for temperature and relative humidity a sinusoidal progression was assumed, with maxima and minima at dawn and 3 h after solar noon, respectively. In addition, daily precipitation sums were uniformly distributed over 24 h, and wind speed was assumed constant at 1 m s^{-1} .

The quality of the hourly data was tested indirectly by assessing their impact on the model results. With respect to the simulation of productivity and fluxes of C, N and water at Oensingen (data not shown), no significant departure from the baseline runs (see 'Results') was found.

2.5. Simulations with climate scenarios. Climate scenarios for 1991–2100 were developed on the basis of climate projections for the 2100s derived from the

output of the Climate High-Resolution Model (CHRM, Vidale et al. 2003). The data were obtained from the archives of the PRUDENCE project (Christensen & Christensen 2007) and refer to the A2 emissions scenario (IPCC 2000).

The relevant monthly anomalies are presented in Table 1. Apart from a temperature increase on the order of 3°C in winter and 5°C in summer, the most striking feature of the scenario is the marked decrease in rainfall amounts during May–November and concurrent increase in the duration of dry spells. With respect to the summer season (Fig. 1), the scenario suggests a more frequent occurrence of heat and water stress comparable to the conditions observed during the summer heat wave of 2003 (Schär et al. 2004).

Given the implications of drought for the ecosystem dynamics under the working hypothesis that clover is less tolerant of water stress than grass, 3 scenarios were generated to study the consequences of drought as a single factor, and in combination with changes in temperature, radiation and atmospheric CO₂ concentrations. These were: (1) a growing-season drought scenario (GSD) defined only by changes in rainfall amounts and duration of wet and dry spells during April to October as given in Table 1; (2) a full A2 climate change scenario, but with CO₂ concentration kept constant at 370 ppm (A2-370); and (3) a full A2 climate change scenario with increasing CO₂ concentration as defined by the Bern-CC model (Appendix II in IPCC 2001) with a value of 860 ppm by the end of the century (A2-860).

For each scenario, a total of 10 individual realizations of 110 yr of daily synthetic weather were created with

Table 1. Changes (Δ) in monthly climate statistics between 2071–2100 and 1961–1990 simulated by the Climate High Resolution Model for the Swiss Plateau under the assumption of an A2 emissions scenario. Changes in mean precipitation rate (P), duration of wet (τ_{wet}) and dry (τ_{dry}) spells, global radiation (GR) and interannual standard deviation of air temperature (σ_T) are relative; changes in daily maximum (T_{max}) and minimum (T_{min}) air temperature are absolute

Month	ΔP	$\Delta \tau_{\text{wet}}$	$\Delta \tau_{\text{dry}}$	ΔT_{max} (°C)	ΔT_{min} (°C)	$\Delta \sigma_T$	ΔGR
Jan	1.10	0.91	0.65	3.51	3.07	0.80	1.07
Feb	1.44	1.19	0.73	2.57	2.11	0.79	0.98
Mar	1.26	1.01	0.70	1.93	1.38	0.96	1.00
Apr	0.99	0.86	1.11	2.99	2.15	1.18	1.14
May	0.77	0.53	1.23	3.58	2.49	1.11	1.16
Jun	0.72	0.72	1.75	4.07	2.89	1.33	1.13
Jul	0.53	0.77	2.21	5.64	3.49	1.23	1.14
Aug	0.69	0.75	1.79	7.05	4.28	1.13	1.17
Sep	0.72	0.86	1.34	5.95	4.00	1.00	1.12
Oct	0.98	0.81	1.08	4.40	3.00	1.11	1.16
Nov	0.66	0.82	1.34	3.39	1.64	0.96	1.32
Dec	1.06	1.15	0.92	3.37	2.58	0.79	1.23

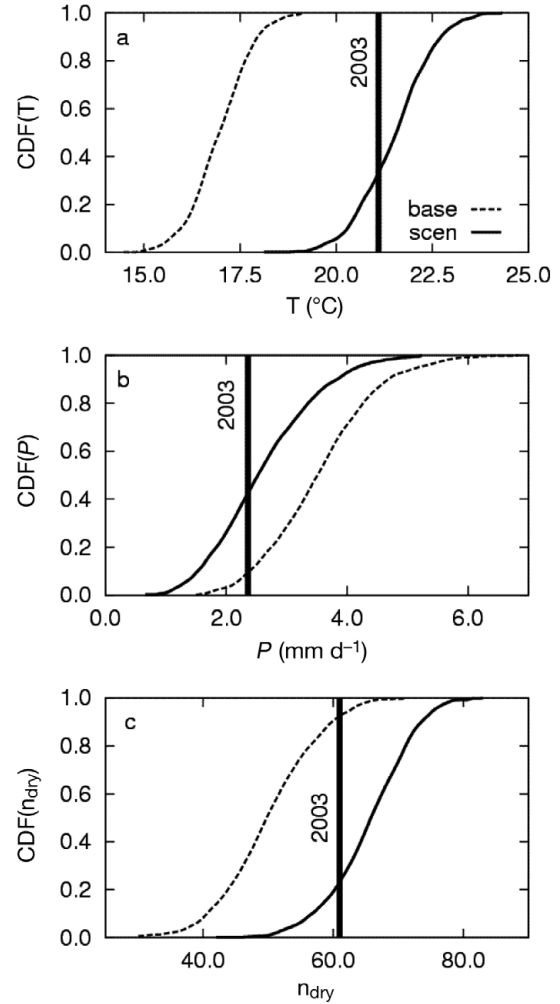


Fig. 1. Cumulative distribution functions (CDFs) of June–July–August average values for (a) daily temperature (T), (b) precipitation rate (P) and (c) number of dry days (n_{dry}) under current climatic conditions (dashed lines) and as projected by the A2-860 scenario (solid lines). The CDFs were estimated from data spanning a 30 yr period (1961–1990 and 2071–2100). Observed mean values during the summer of 2003 are included for comparison (thick vertical line)

LARS-WG. (Daily values of the minimum/maximum relative humidity, currently not part of the standard output of LARS-WG, were calculated from solar radiation using statistical relations fitted to the observations for each month of the year and assumed valid also under altered climatic conditions.) Although a larger number of realizations would have been desirable for a quantitative assessment of scenario uncertainties, our practical choice nevertheless offered the opportunity to explore the range of solutions admitted by the statistical properties of the local climate and the climate anomalies.

Model simulations were started in 1991 assuming a constant management with 3 annual harvests at fixed

dates and without application of N fertilizers, in agreement with the current practices at Oensingen. In view of the rapid changes during establishment of the sward in the first few years after sowing (see also Lazzarotto et al. 2009), the years 1991 to 2000 were disregarded from the analysis.

3. RESULTS

3.1. Model performance

The model performance for current conditions was assessed by comparing simulated and measured multi-year data of aboveground biomass, clover biomass fraction and net ecosystem CO₂ exchange (NEE). Initial conditions for SOM pools were the same as used by Lazzarotto et al. (2009) and the timing of harvests was obtained from the log files of the field experiment.

With a few exceptions, simulation results for the selected parameters were consistent with measurements (Fig. 2), implying that the model was able to capture essential aspects of biomass dynam-

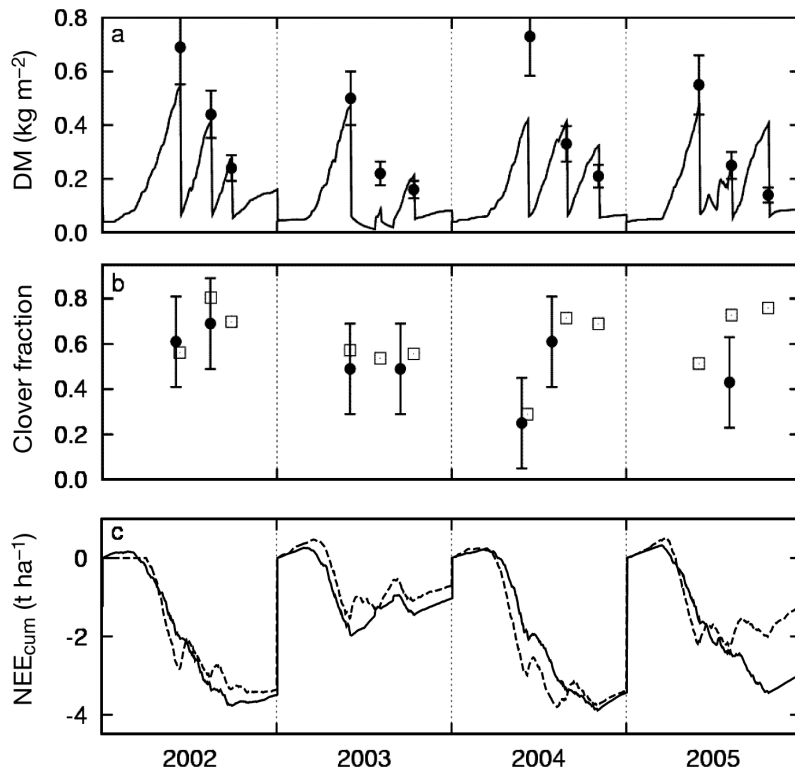


Fig. 2. Performance of PROGRASS in simulating (a) aboveground dry-matter (DM) production, (b) clover fraction and (c) cumulative net ecosystem exchange (NEE_{cum}) on the extensively managed field in Oensingen, 2002–2005. Continuous lines and empty squares: simulation results; closed circles and dashed lines: observations; error bars: SD

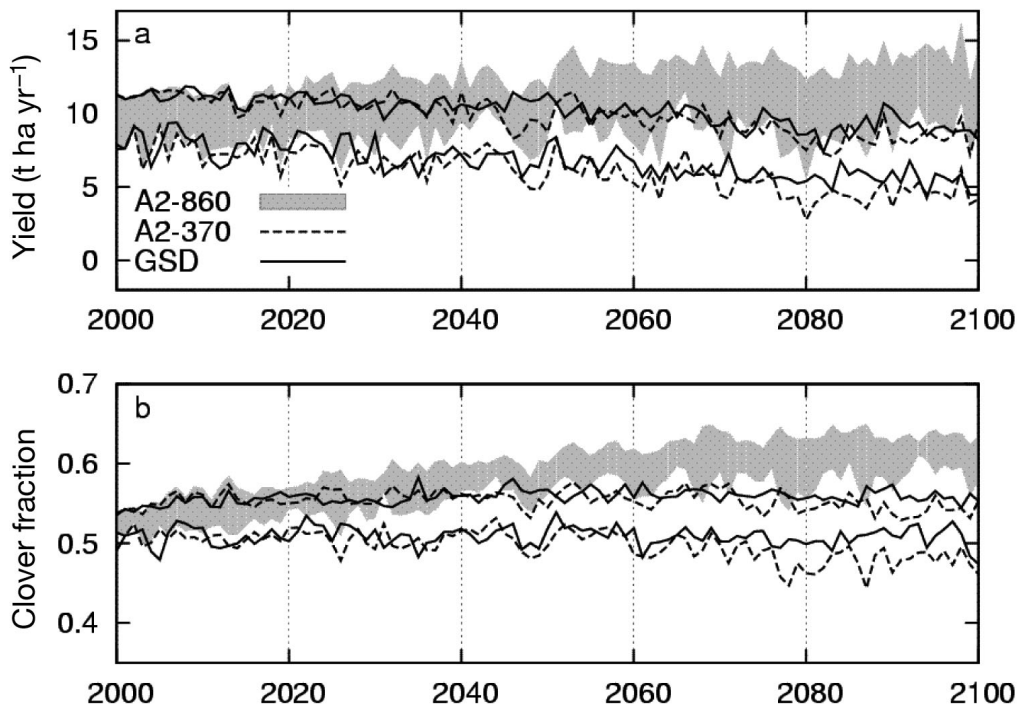


Fig. 3. Transient simulations for the 21st century of (a) annual yield and (b) annual mean clover fraction for the growing-season drought (GSD, solid lines), A2-370 (dashed lines) and A2-860 (grey area) scenarios. For each scenario, the range of mean \pm SD from 10 simulations driven by independent LARS-WG realizations of the daily weather is given

ics such as seasonal patterns and interannual variation during a period with strongly variable climatic conditions including the 2003 drought. For aboveground biomass (Fig. 2a), the root mean square difference (RMSD) between observations and simulations was $0.14 \text{ kg DM m}^{-2}$ and the largest discrepancies were found for reproductive growth and the last regrowth period in 2006. For the latter, the model also overestimated the clover fraction (Fig. 2b)—reasons for this discrepancy were already discussed in Lazzarotto et al. (2009)—but, given a RMSD of 0.14, the results can be considered as satisfactory.

For cumulative NEE, the RMSD was 0.59 tonnes (t) ha^{-1} . However, most of the time simulations matched measurements better than indicated by the statistics, and substantial discrepancies were mostly restricted to the second half of 2005 (Fig. 2c). Additional analysis of the component fluxes of NEE (not shown) suggested that these latter differences were likely due to overes-

timination of ecosystem respiration during a short period of about 15 d following the second harvest.

3.2. Projection of changes in yield and clover fraction

Annual yields decreased from about 10.0 t ha^{-1} under present climatic conditions to 7.0 and 6.5 t ha^{-1} under GSD and A2-370 scenarios, respectively, by the end of the century (Fig. 3a). In contrast, under the A2-860 scenario, annual yields increased to nearly 12.0 t ha^{-1} as a result of increasing clover fraction (Fig. 3b) and clover productivity (data not shown). Clover fraction increased from about 0.55 in 2001 to nearly 0.60 in 2080, remaining at this level thereafter. Little changes in clover fraction were found under the GSD scenario, whereas a statistically significant negative trend resulted from the A2-370 scenario over the entire time period.

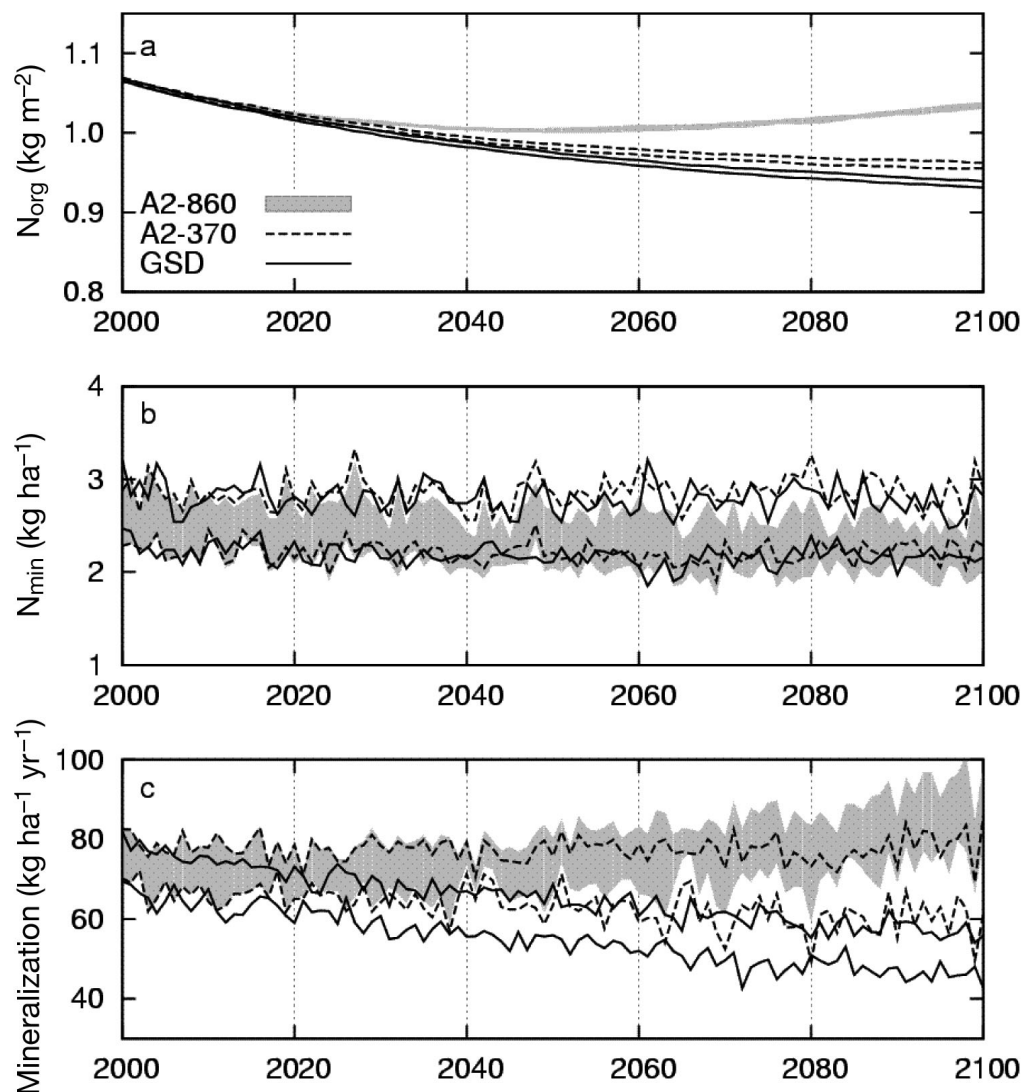


Fig. 4. Same as Fig. 3 but for (a) soil organic N stock (N_{org}), (b) soil mineral N stock (N_{min}) and (c) net mineralization rate

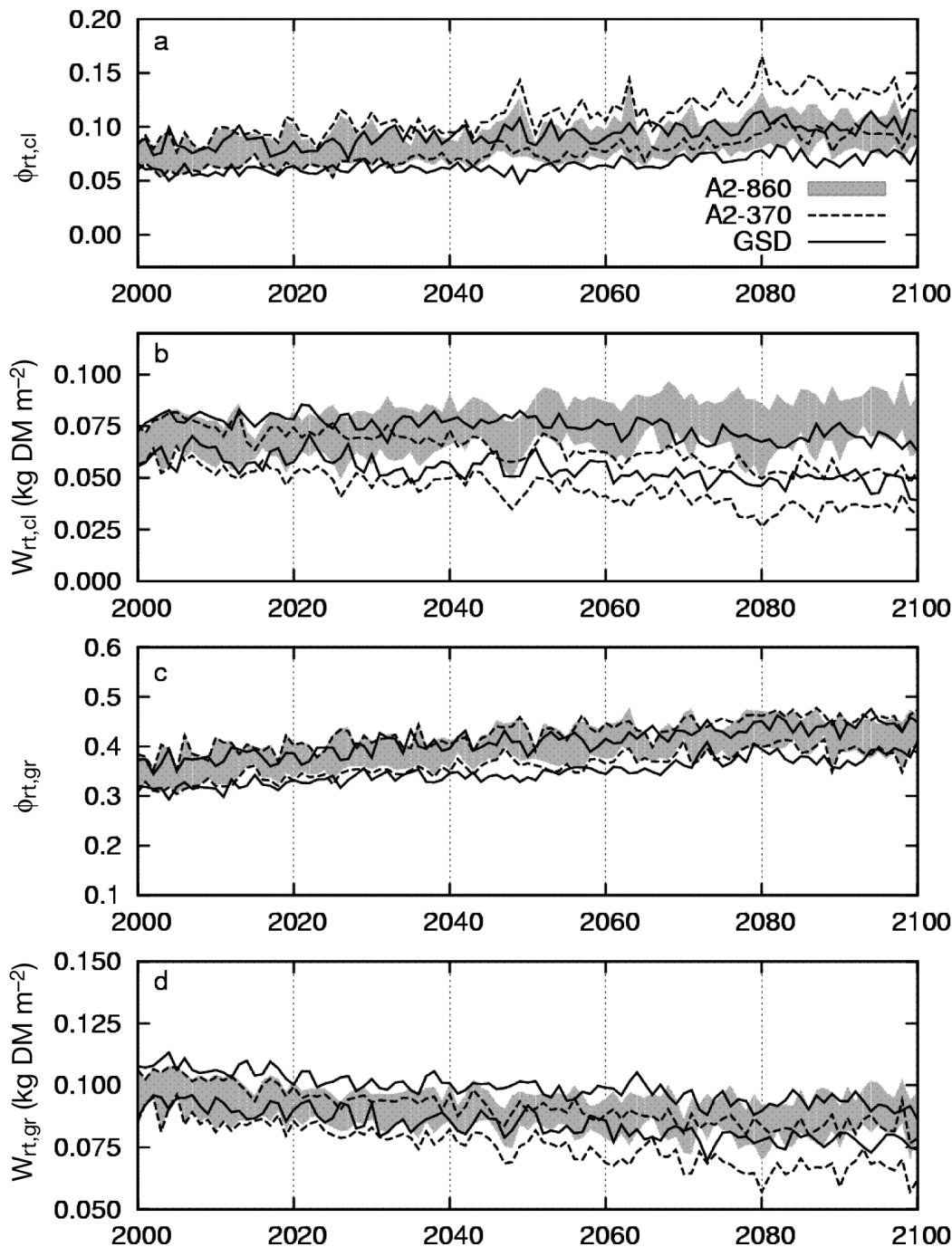


Fig. 5. Same as Fig. 3 but for (a, c) annual mean fraction of assimilates allocated to roots ($\phi_{rt,cl}$, $\phi_{rt,gr}$) and (b, d) total root biomass ($W_{rt,cl}$, $W_{rt,gr}$). Subscripts cl and gr denote white clover *Trifolium repens* L. and perennial ryegrass *Lolium perenne* L., respectively

3.3. Projection of changes in soil N stocks and net mineralization

For all scenarios, soil organic N stocks dropped rapidly during the initial phase of the simulations (Fig. 4a), with an initial loss rate of approximately $20 \text{ kg N ha}^{-1} \text{ yr}^{-1}$ that is consistent with the experimental findings of Ammann et al. (2009) at our study site. This suggested an imbalance between the loss caused by

net mineralization (about $80 \text{ kg N ha}^{-1} \text{ yr}^{-1}$ under present climatic conditions) and the input from plant litter (roughly $60 \text{ kg N ha}^{-1} \text{ yr}^{-1}$), which continued until about 2030 under A2-860 and 2050 under GSD and A2-370. Later, the negative trend in organic N stock was reversed under A2-860, and slowed down under GSD and A2-370 as a result of either increasing sward productivity (A2-860) (Fig. 3a) or decreased net mineralization (GSD, in particular) (Fig. 4c). Regarding soil

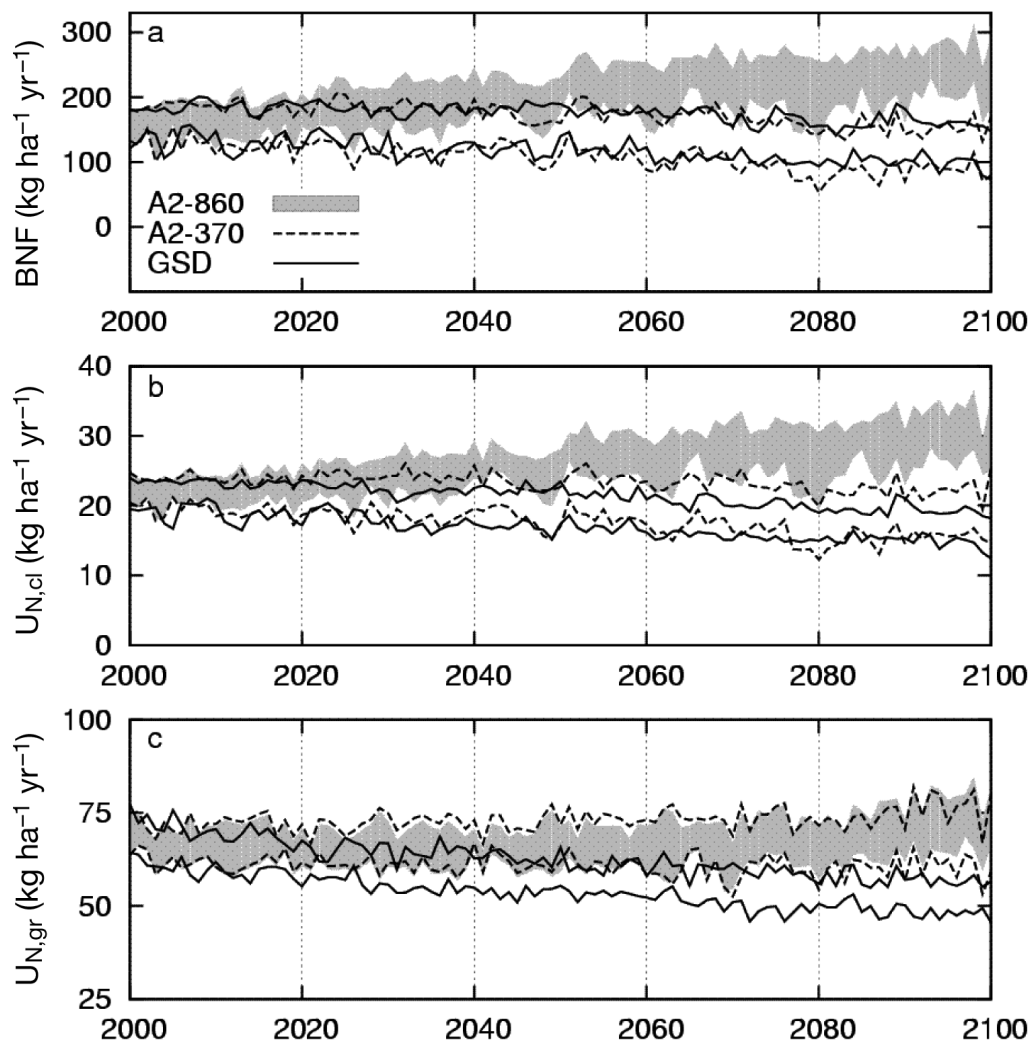


Fig. 6. Same as Fig. 3 but for (a) annual mean biological N_2 fixation (BNF) and (b, c) annual mean uptake of soil mineral N by white clover *Trifolium repens* ($U_{N,cl}$) and ryegrass *Lolium perenne* ($U_{N,gr}$), respectively

mineral N, regression analysis revealed a weak but statistically significant negative long-term trend, with a total decline of 5% under GSD and 12% under A2-860 (Fig. 4b). Under A2-370, soil mineral N stock remained unchanged.

3.4. Projection of changes in root biomass, BNF and N uptake

Allocation of assimilates to roots increased with time in all 3 scenarios, both for grass and clover (Fig. 5a,c). Yet an increase in root biomass was only found in clover under the A2-860 scenario, and root biomass in clover decreased under the 2 other scenarios, most strongly under the assumption of constant CO_2 (A2-370) (Fig. 5b). For grass, a decline in root biomass was found with all scenarios (Fig. 5d), reflecting a stronger limitation of C assimilation and a decrease in total productivity (data not shown).

BNF was clearly stimulated by elevated CO_2 (Fig. 6a), although with increasing variability, whereas in the absence of CO_2 stimulation (GSD and A2-370) BNF tended to decrease during the second half of the simulation period (Fig. 6a). The pattern of N uptake in clover for the different scenarios was similar to those of BNF (Fig. 6b). For the grass component, N uptake remained stable under both A2 scenarios, but it declined under GSD (Fig. 6c).

4. DISCUSSION

Differences in the response to environmental drivers between legumes and grasses can be expected from experimental data (Lüscher et al. 2005). With respect to C assimilation and growth, clover was assumed less tolerant of drought than grass, and we therefore hypothesized that climate change associated with more frequent soil water deficits could ultimately lead

to a continuous decline in clover abundance. In the absence of CO₂ stimulation (A2-370), a slightly negative trend in clover fraction was indeed observed (Fig. 3b).

On the other hand, clover biomass and total sward productivity (Fig. 3a) were found to benefit from elevated CO₂ (A2-860), in agreement with findings by Hebeisen et al. (1997). In the absence of nutrient limitations, positive effects of elevated CO₂ are generally observed in legumes (Rogers et al. 2006) and can be attributed to increased C availability (Hu et al. 2006). In the model, this was accounted for by enhanced photosynthesis and BNF. Given the concurrent decline in productivity of grass (data not shown), our findings agree with the conclusion by Zanetti et al. (1996) that in grass–clover mixtures, yield stimulation by elevated CO₂ results primarily from an increase in clover productivity.

The positive trend observed under A2-860 could also result from improved drought tolerance of N₂ fixation (Serraj et al. 1998). In PROGRASS this was implemented as an increase in the minimal BNF rate (Eq. 4) and a reduction in the soil water content at which BNF starts to be limited by water stress (Eq. 5). However, sensitivity tests (data not shown) suggested that in our case study this effect was of minor importance.

We also noticed that the positive CO₂ effect could persist even on a background of increasing temperatures beyond time scales of a few years, which are typical for field experiments (Figs. 3 & 6, in particular). This suggests that unless water becomes limiting for BNF, sward productivity in unfertilized grassland ecosystems could be sustained under increasing CO₂ in spite of a higher incidence of heat stress. In the absence of CO₂ stimulation (A2-370), however, BNF was found to decline over time (Fig. 6a), leading to a significant reduction in sward productivity (Fig. 3a).

In the Swiss FACE experiment, root mass of perennial ryegrass showed a marked positive response to elevated CO₂ (Hebeisen et al. 1997). This could have implications for the composition of the sward, as in another application of PROGRASS Lazzarotto et al. (2009) noticed that more vigorous root growth in grass could provide competitive advantages in terms of N acquisition and positive feedbacks on C assimilation and light interception. However, this type of response could not be found in our simulations, despite a relative increase in the allocation of assimilates to grass roots (Fig. 5c). Likely this reflected the limited soil mineral N availability (of the order of 2.5 kg ha⁻¹ throughout the simulation period), which is in contrast with the 100 kg N ha⁻¹ yr⁻¹ applied even to the low N plots in the FACE experiment.

Overall, the simulations underlined the role of BNF as a key element of grassland dynamics. However,

BNF appears here in a somewhat different light than in the modelling study conducted by Thornley & Cannell (2000). While the size of the soil mineral N pool is primarily determined by the turnover of SOM, here the annual system N gain through BNF was on the order of 100 to 300 kg N ha⁻¹ yr⁻¹, exceeding the input from net mineralization (i.e. the balance between gross mineralization and immobilization), which was less than 100 kg N ha⁻¹ yr⁻¹. Although not examined in detail, this result suggests a stronger impact of increasing temperatures and decreasing soil water availability on mineralization than on BNF, underpinning the need for a better understanding of the interactions between soil and vegetation in the context of climate change.

5. CONCLUSIONS

We developed transient climate scenarios that project strongly increasing temperatures and more extended drought periods during late spring, summer and early autumn. These trends affect nutrient cycling and productivity of grass–clover swards, but the net effect strongly depends on the concurrent increase in CO₂, to which legumes may respond more strongly than grasses. With respect to the initial hypotheses, the following conclusions were drawn:

(1) Clover abundance did not decline even in the absence of CO₂ stimulation, because BNF was less severely affected by increasing heat and water stress than N uptake in grass.

(2) A decrease in clover abundance was also prevented because root growth in clover was less strongly limited by climate change than in grass. As a consequence, grass could not obtain competitive advantages with respect to N acquisition, C assimilation and light interception.

(3) Clover development benefited from the overall positive effects of CO₂ on N acquisition, in particular improved drought tolerance of BNF.

Overall, the positive response of BNF to elevated CO₂ was the reason for increasing productivity of the sward. This result is broadly consistent with experimental observations. However, its general validity remains to be demonstrated. Also, in extending the present analysis, the implications of recent experiments on the combined effects of higher temperature, water stress and elevated CO₂ on C assimilation and growth of fixing legumes (Aranjuelo et al. 2008, 2009) should be taken into account.

In addition, we did not consider possible changes in plant traits and soil microbial biomass activity, which reflect the genetic plasticity of plants and soil organisms and could be induced either through acclimation or breeding. Such changes could significantly alter the

ecosystem responses to the combined effects of climate change and elevated CO₂. Finally, it is likely that technical progress in the management of grasslands and pastures will overcome some of the impacts brought about by increasing temperatures and drought.

Acknowledgements. The authors wish to acknowledge the financial support of the National Centre of Competence in Research on Climate (NCCR Climate) and the EU project NitroEurope IP (contract no. 017841-2). We are also grateful to the Swiss Federal Office of Meteorology and Climatology for granting access to its database. Regional climate simulations with CHRM were obtained from the data archive of the PRUDENCE project (funded by the EU through contract no. EVK2-CT2001-00132). Rothamsted Research receives grant-aided support from the Biotechnology and Biological Sciences Research Council (BBSRC) of the United Kingdom. Comments by 4 anonymous reviewers helped to substantially improve the manuscript.

LITERATURE CITED

- Ammann C, Spirig C, Leifeld J, Neftel A (2009) Assessment of the nitrogen and carbon budget of two managed temperate grassland fields. *Agric Ecosyst Environ* 133: 150–162
- Aranjuelo I, Irigoyen JJ, Sánchez-Díaz M, Nogués S (2008) Carbon partitioning in N₂ fixing *Medicago sativa* plants exposed to different CO₂ and temperature conditions. *Funct Plant Biol* 35:306–317
- Aranjuelo I, Irigoyen JJ, Nogués S, Sánchez-Díaz M (2009) Elevated CO₂ and water-availability effect on gas exchange and nodule development in N₂-fixing alfalfa plants. *Environ Exp Bot* 65:18–26
- Braun-Blanquet J (1964) *Grundzüge der Vegetationskunde*, 3rd edn. Springer, Berlin
- Campbell GS (1985) *Soil physics with BASIC*. Transport models for soil–plant systems. *Developments in Soil Science* 14. Elsevier Science Publishers, Amsterdam
- Carslaw HS, Jaeger JC (1959) *Conduction of heat in solids*, 2nd edn. Oxford University Press, Oxford
- Christensen JH, Christensen OB (2007) A summary of the PRUDENCE model projections of changes in European climate by the end of this century. *Clim Change* 81:7–30
- Conant RT, Paustian K, Del Grosso SJ, Parton WJ (2005) Nitrogen pools and fluxes in grassland soils sequestering carbon. *Nutr Cycl Agroecosyst* 71:239–248
- Davies JA (1967) A note on the relationship between net radiation and solar radiation. *Q J R Meteorol Soc* 93:109–115
- de Graaff MA, van Groenigen KJ, Six J, Hungate B, van Kessel K (2006) Interactions between plant growth and soil nutrient cycling under elevated CO₂: a meta-analysis. *Global Change Biol* 12:2077–2091
- Diaz S, Grime JP, Harris J, McPherson E (1993) Evidence of a feedback mechanism limiting plant response to elevated carbon dioxide. *Science* 364:616–617
- Frame J, Newbould P (1986) Agronomy of white clover. *Adv Agron* 40:1–88
- Hebeisen T, Lüscher A, Zanetti S, Fischer BU and others (1997) Growth response of *Trifolium repens* L. and *Lolium perenne* L. as monocultures and bi-species mixture to free air CO₂ enrichment and management. *Global Change Biol* 3:149–160
- Holtslag AAM, van Ulden AP (1983) A simple scheme for daytime estimates of the surface fluxes from routine weather data. *J Clim Appl Meteorol* 22:517–529
- Hu S, Tu C, Chen X, Gruver JB (2006) Progressive N limitation of plant response to elevated CO₂: a microbiological perspective. *Plant Soil* 289:47–58
- Hunt HW, Trlica MJ, Redente EF, Moore JC and others (1991) Simulation model for the effects of climate change on temperate grassland ecosystems. *Ecol Model* 53:205–246
- Hunt HW, Morgan JA, Read JJ (1998) Simulating growth and root-shoot partitioning in prairie grasses under elevated atmospheric CO₂ and water stress. *Ann Bot* 81:489–501
- IPCC (2000) *Special Report on Emissions Scenarios*. Nakicenovic N, Swart R (eds) Cambridge University Press, Cambridge
- IPCC (2001) *Climate change 2001: the scientific basis*. Contribution of Working Group I to the third assessment report of the Intergovernmental Panel on Climate Change. Cambridge University Press, Cambridge
- Jobbágy EG, Jackson RB (2000) The vertical distribution of soil organic carbon and its relation to climate and vegetation. *Ecol Appl* 10:423–436
- Lazzarotto P, Calanca P, Fuhrer J (2009) Dynamics of grass–clover mixtures—an analysis of the response to management with the PROductive GRASSland Simulator (PROGRASS). *Ecol Model* 220:703–724
- Long SP, Ainsworth EA, Leakey ADB, Nösberger J, Ort DR (2006) Food for thought: lower-than-expected crop yield stimulation with rising CO₂ concentrations. *Science* 312: 1918–1921
- Louie K, Graeme CW, Lambert G, MacKay A, Barker D (2002) A delay model for the growth of ryegrass–clover mixture: formulation and preliminary simulations. *Ecol Model* 155:31–42
- Lüscher A, Fuhrer J, Newton PCD (2005) Global atmospheric change and its effect on managed grassland systems. In: McGilloway DC (ed) *Grassland: a global resource*. Wageningen Academic Publishers
- Monteith JL, Szeicz G (1961) The radiation balance of bare soil and vegetation. *Q J R Meteorol Soc* 87:159–170
- Parton WJ, Schimel DS, Cole CV, Ojima DS (1987) Analysis of factors controlling soil organic matter levels in Great Plains grasslands. *Soil Sci Soc Am J* 51:1173–1179
- Parton WJ, Scurlock JMO, Ojima DS, Gilmanov TG and others (1993) Observations and modeling of biomass and soil organic matter dynamics for the grassland biome worldwide. *Global Biogeochem Cycles* 7:785–809
- Parton WJ, Scurlock JMO, Ojima DS, Schimel DS and others (1995) Impact of climate change on grassland production and soil carbon worldwide. *Global Change Biol* 1:13–22
- Racsko P, Szeidl L, Semenov M (1991) A serial approach to local stochastic weather models. *Ecol Model* 57:27–41
- Rastetter EB, Agren GI, Shaver GR (1997) Responses of N-limited ecosystems to increased CO₂: a balanced-nutrition, coupled-element-cycles model. *Ecol Appl* 7:444–460
- Riedo M, Gyalistras D, Fischlin A, Fuhrer J (1999) Using an ecosystem model linked with GCM-derived local weather scenarios to analyse effects of climate change and elevated CO₂ on dry matter production and partitioning, and water use in temperate managed grasslands. *Global Change Biol* 5:213–223
- Rogers A, Gibon Y, Stitt M, Morgan PB, Bernacchi CJ, Ort DR, Long SP (2006) Increased C availability at elevated carbon dioxide concentration improves N assimilation in a legume. *Plant Cell Environ* 29:1651–1658
- Ross PJ, Henzell EF, Ross DR (1972) Effects of nitrogen and light in grass-legume pastures. A systems analysis approach. *J Appl Ecol* 9:535–556

- Schaap MG, Leij FJ, van Genuchten MT (2001) ROSETTA: a computer program for estimating soil hydraulic parameters with hierarchical pedotransfer functions. *J Hydrol* 251:163–176
- Schär C, Vidale PL, Lüthi D, Frei C, Häberli C, Liniger MA, Appenzeller C (2004) The role of increasing temperature variability in European summer heatwaves. *Nature* 427:332–336
- Schimel DS (1995) Terrestrial ecosystems and the carbon cycle. *Global Change Biol* 1:77–91
- Schneider MK, Lüscher A, Richter M, Aeschlimann U and others (2004) Ten years of free-air CO₂ enrichment altered the mobilization of N from soil in *Lolium perenne* L. swards. *Global Change Biol* 10:1377–1388
- Schulte RPO (2003) Analysis of the production stability of mixed grasslands. II. A mathematical framework for the quantification of production stability in grassland ecosystems. *Ecol Model* 159:71–99
- Schulte RPO, Lantinga EA, Struik PC (2003) Analysis of the production stability of mixed grasslands. I. A conceptual framework for the qualification of production stability in grassland ecosystems. *Ecol Model* 159:43–69
- Schwinning S, Parsons AJ (1996a) Analysis of the coexistence mechanisms for grasses and legumes in grazing systems. *J Ecol* 84:799–813
- Schwinning S, Parsons AJ (1996b) A spatially explicit population model of stoloniferous N-fixing legumes in mixed pasture with grass. *J Ecol* 84:815–826
- Semenov MA (2007) Development of high resolution UKCIP02-based climate change scenarios in the UK. *Agric For Meteorol* 144:127–138
- Semenov MA, Barrow EM (1997) Use of a stochastic weather generator in the development of climate change scenarios. *Clim Change* 35:397–414
- Semenov MA, Brooks RJ, Barrow EM, Richardson CW (1998) Comparison of the WGEN and LARS-WG stochastic weather generators for diverse climates. *Clim Res* 10:95–107
- Serraj R, Sinclair TR, Allen LH (1998) Soybean nodulation and N₂ fixation response to drought under carbon dioxide enrichment. *Plant Cell Environ* 21:491–500
- Shaw MR, Zavaleta ES, Chiariello NR, Cleland EE, Mooney HA, Field CB (2002) Grassland responses to global environmental changes suppressed by elevated CO₂. *Science* 298:1987–1990
- Thornley JHM, Cannell MGR (1997) Temperate grassland responses to climate change: an analysis using the Hurley Pasture Model. *Ann Bot* 80:205–221
- Thornley JHM, Cannell MGR (2000) Dynamics of mineral N availability in grassland ecosystems under increased [CO₂]: hypotheses evaluated using the Hurley Pasture Model. *Plant Soil* 224:153–170
- Thornley JHM, France J (2007) *Mathematic models in agriculture*. CAB International, Wallingford
- Thornley JHM, Bergelson J, Parsons AJ (1995) Complex dynamics in a carbon-nitrogen model of a grass-legume pasture. *Ann Bot* 75:79–84
- Topp CFE, Doyle CJ (1996) Simulating the impact of global warming on milk and herbage production in Scotland. 1. The effects on dry-matter yield of grass and grass-white clover swards. *Agric Syst* 52:213–242
- Vidale PL, Lüthi D, Frei C, Seneviratne S, Schär C (2003) Predictability and uncertainty in a regional climate model. *J Geophys Res* 108:4586
- Volk M, Niklaus PA, Körner C (2000) Soil moisture effects determine CO₂ responses of grassland species. *Oecologia* 125:380–388
- Whitehead DC (1995) *Grassland nitrogen*. CAB International, Wallingford
- Zanetti S, Hartwig UA, Lüscher A, Hebeisen T and others (1996) Stimulation of symbiotic N₂ fixation in *Trifolium repens* L. under elevated atmospheric pCO₂ in a grassland ecosystem. *Plant Physiol* 112:575–583

Editorial responsibility: Gerrit Hoogenboom, Griffin, Georgia, USA

*Submitted: May 20, 2009; Accepted: January 28, 2010
Proofs received from author(s): April 21, 2010*